Gravitational Waves from Compressible MHD Turbulence in Cosmological Phase Transitions

1. Gravitational wave equation with sources
2. MHD turbulence and time correlations
3. Gravitational waves from MHD turbulence in phase transitions
4. Summary and Outlook

partly based on Niksa, Schlederer, Sigl, CQG 35 (2018) 144001 [arXiv:1803.02271]

DFG Deutsche Forschungsgemeinschaft

PROJEKTTRÄGER FÜR DAS Bundesministerium für Bildung und Forschung

Universität Hamburg
DER FORSCHUNG | DER LEHRE | DER BILDUNG

Günter Sigl
II. Institut theoretische Physik, Universität Hamburg

Introduction

(Incomplete) list of the relevant literature:

- Kamionkowski et al 1994: bubble collisions can produce turbulence which contributes to gravitational waves
- Kosowsky et al 2002: extension beyond quadrupole approximation, contribution from Kolmogorov tail, no turbulence decay
- Dolgov et al 2002: no turbulence decay, $k^{-7/2}$
- Kahniashvili et al 2008a, 2008b: helical MHD turbulence, temporal decor relation in Lagrangian frame
- Caprini et al 2009: turbulent decay, unequal time correlations in Lagrangian frame, problem of negative gravitational wave spectra, $k^{-5/3}$
- Hindmarsh et al 2015, 2017: compressional hydro simulations, gravitational wave spectrum k^5 and k^{-3} above and below bubble separation scale, respectively, with some dependence of bubble wall velocity
- Roper Pol et al 2019: MHD turbulence simulations
- Cutting et al. 2019: for deflagrations in strong transitions kinetic energy and gravitational wave power is reduced

Reminder [see, e.g. Caprini and Figueroa review CQG 35 (2018) 163001]:

$\rho_{GW} \sim (\partial_\tau h)^2/G_N \sim G_N \Pi^2/\beta^2$, so that with $\rho_{\rm tot} \sim H^2/G_N$ one has

$$\frac{\rho_{GW}}{\rho_{\rm tot}} \sim \left(\frac{H_*}{\beta}\right)^2 \left(\frac{\Pi}{\rho_{\rm tot}^*}\right)^2 \sim \left(\frac{H_*}{\beta}\right)^2 \left(\frac{\kappa\alpha}{1+\alpha}\right)^2,$$

with $\kappa \equiv \Pi/L$ and $\alpha \equiv L/\rho_r$ in terms of the latent heat L. Since sound waves last longer than bubbles by a factor $\sim \beta/H_*$, their contribution may dominate.
=> motivation to concentrate on MHD turbulence/sound waves.

focus in our work on temporal decorrelation in Eulerian frame in which gravitational wave production is evaluated

also uses various models of decay of dilatational modes semi-analytic

integration of resulting equations for gravitational wave power spectrum

Gravitational Waves with Sources

The gravitational wave equation for the transverse traceless strain and energy momentum tensor in conformal time reads

$$\left(\partial_\tau^2 + 2\mathscr{H}\partial_\tau + k^2\right) h_{ij}(\mathbf{k},\tau) = 16\pi G_{\mathrm{N}}\pi_{ij}(\mathbf{k},\tau)\,,$$

with $\mathscr{H} = \partial_\tau a/a$. The gravitational wave energy density is an average of the conformal time derivative over several wavelengths,

$$\rho_G(\mathbf{r},\tau) \equiv \frac{1}{32\pi G_{\mathrm{N}} a^2(\tau)} \sum_{ij} \left\langle \partial_\tau h_{ij}(\mathbf{r},\tau)\partial_\tau h_{ij}(\mathbf{r},\tau) \right\rangle\,.$$

Normalising to the critical density and assuming spherical symmetry we use the convention

$$\Omega_{GW}(\tau) = \int d\ln(k)\Omega_G(k,\tau)$$

The energy-momentum tensor due to magnetic field can be written as

$$\pi^B_{ij}(\mathbf{k},\tau) = P^2_{ij,kl}T^{\rm em}_{kl}(\mathbf{k},\tau) = \frac{1}{2(2\pi)^4}P^2_{ij,kl}\int d^3\mathbf{q}\, B_i(\mathbf{q},\tau)B_j(\mathbf{k}-\mathbf{q},\tau)\,,$$

where the projector is given by

$$P^2_{ij,lm} = P_{il}(\mathbf{k})P_{jm}(\mathbf{k}) - \frac{1}{2}P_{ij}(\mathbf{k})P_{lm}(\mathbf{k})\,,$$

with $P_{jm}(\mathbf{k}) = \delta_{jm} - k_j k_m/k^2$.

With the Alfven velocity components $b_i = B_i/\left[4\pi(\rho+p)\right]^{1/2}$ the magnetic field correlators are taken as follows:

$$\left\langle b_i(\mathbf{k},\tau)b^*_j(\mathbf{q},\tau)\right\rangle = \frac{(2\pi)^6}{4\pi k^3}\delta^3(\mathbf{k}-\mathbf{q})\left[P_{ij}(\mathbf{k})E_B(\mathbf{k},\tau) - i\epsilon_{ijl}\frac{k^l}{k}h_B(\mathbf{k},\tau)\right]\,,$$

with the magnetic field energy density

$$\rho_B = (\rho + p)\int d^3\mathbf{k}\frac{\langle \mathbf{b}(\mathbf{k})\cdot\mathbf{b}(-\mathbf{k})\rangle}{2(2\pi)^3} = (\rho + p)\int d\ln(k)E_B(k)\,,$$

and the magnetic helicity density

$$H_B = \int \frac{d^3\mathbf{k}}{(2\pi)^6}\langle \mathbf{A}(\mathbf{k})\cdot\mathbf{B}(-\mathbf{k})\rangle = i\int \frac{d^3\mathbf{k}}{(2\pi)^6 k^2}\langle (\mathbf{k}\times\mathbf{B}(\mathbf{k}))\cdot\mathbf{B}(-\mathbf{k})\rangle$$
$$= \int d\ln(k)\frac{(\rho+p)}{k}h_B(k)\,.$$

Similarly for the kinetic component

$$\left\langle v_i(\mathbf{k},\tau)v_j^*(\mathbf{q},\tau)\right\rangle = \frac{(2\pi)^6}{4\pi k^3}\delta^3(\mathbf{k}-\mathbf{q})\Bigg[\left(\delta_{ij}-\frac{k_ik_j}{k^2}\right)E_S(\mathbf{k},\tau)+$$
$$2\frac{k_ik_j}{k^2}E_D(\mathbf{k},\tau) - i\epsilon_{ijl}\frac{k^l}{k}h_V(\mathbf{k},\tau)\Bigg]\,,$$

with $E_S(\mathbf{k},\tau)$ and $E_D(\mathbf{k},\tau)$ the solenoidal (incompressible) and dilatational (compressible) energy spectra and the velocity field energy density

$$\rho_V = (\rho + p)\int d^3\mathbf{k}\frac{\langle \mathbf{v}(\mathbf{k})\cdot\mathbf{v}(-\mathbf{k})\rangle}{2(2\pi)^3} = (\rho+p)\int d\ln(k)\big[E_S(k)+E_D(k)\big]\ ,$$

and the magnetic helicity density

$$H_V = i\int \frac{d^3\mathbf{k}}{(2\pi)^6}\langle(\mathbf{k}\times\mathbf{v}(\mathbf{k}))\cdot\mathbf{v}(-\mathbf{k})\rangle = \int d\ln(k)\frac{(\rho+p)}{k}h_V(k)\,.$$

As a first approximation, we do not need to treat long term MHD turbulence evolution over many Hubble times since the gravitational wave signal will be dominated by the earliest times.

Turbulence Basics

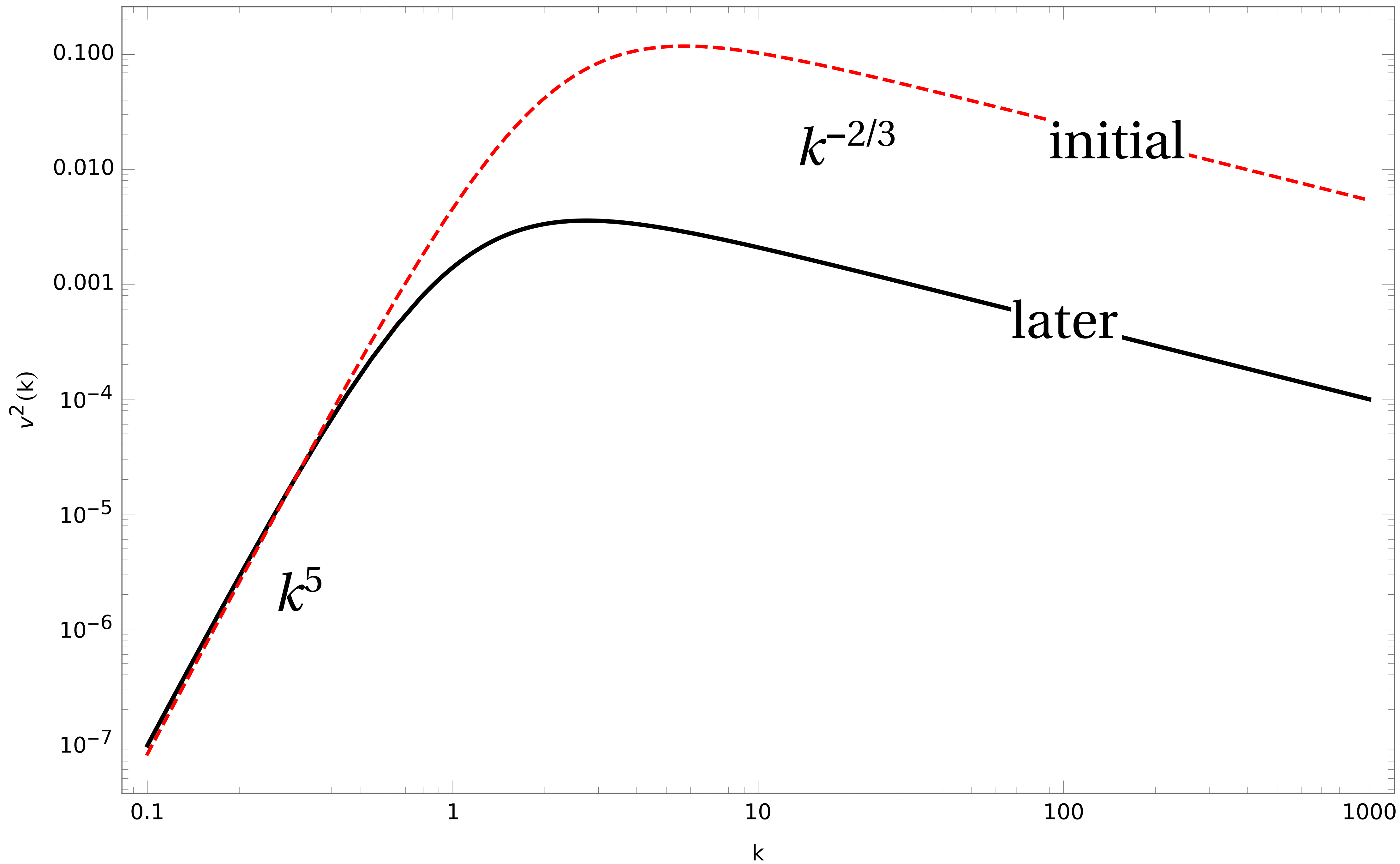

MHD turbulence and time correlations

In the random sweeping approximation one has advection of small scale fluctuations by a random but time-invariant large scale velocity field $\mathbf{U}$,

$$\partial_t \mathbf{v}(\mathbf{k},t) = -i(\mathbf{k}\cdot\mathbf{U})\mathbf{v}(\mathbf{k},t)$$

which gives

$$\langle \mathbf{v}(\mathbf{k},t)\mathbf{v}(\mathbf{k},t+\Delta t)\rangle = \exp\left(-\frac{1}{2}k^2\left\langle U^2\right\rangle \Delta t^2\right)\left\langle v^2(\mathbf{k},t)\right\rangle = \exp\left[-\frac{1}{2}\left(\frac{\Delta t}{t_E(k)}\right)^2\right]\left\langle v^2(\mathbf{k},t)\right\rangle\ ,$$

where $t_E(k) \sim \left[k\langle U^2\rangle^{1/2}\right]^{-1}$ is the Eulerian eddy turnover time. Important to note that Eulerian turnover time is much shorter than Lagrangian turnover time often used before and scales as k^{-1}:

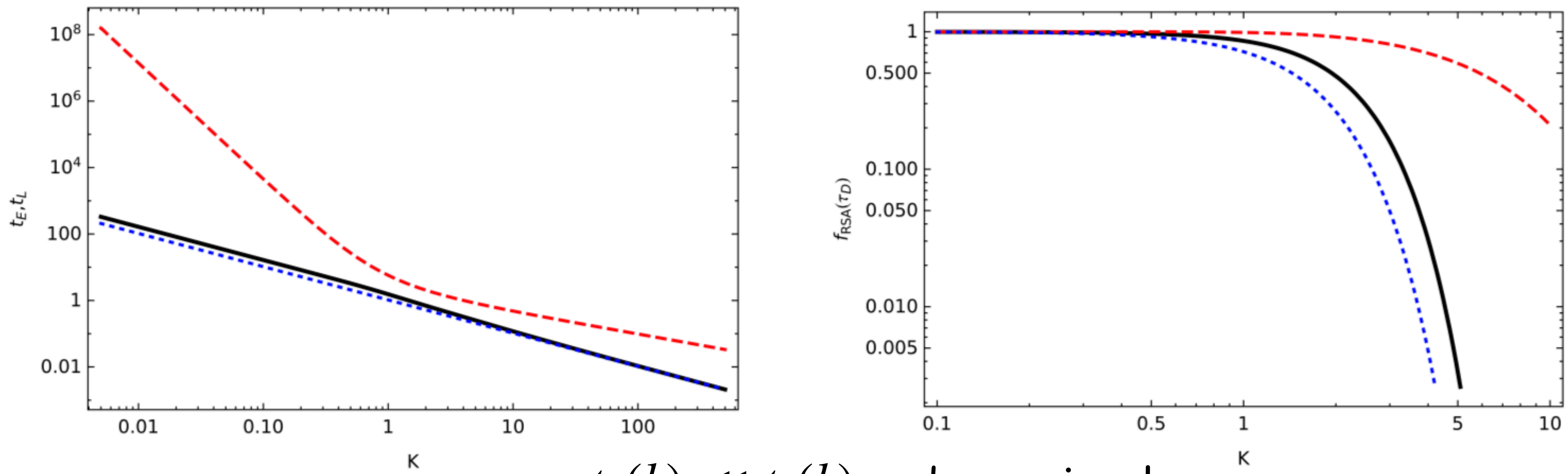

$t_E(k) \ll t_L(k)$ reduces signal

Figure 1. The left panel shows the Lagrangian eddy turnover time (44) (red, dashed) and the Eulerian eddy turnover time based on (53) (black, solid) and based on the $\langle v_1^2 \rangle$ Ansatz (blue, dotted) in arb. units as a function of dimensionless wavenumber $K \equiv kL_I/(2\pi)$. The right panel shows the Gaussian function (50) $f_{\rm RSA}$, evaluated with the decorrelation timescales shown in the left panel with corresponding line and color styles at time $\tau = \tau_{\rm D}$.

$$t_L^{-1}(k) \sim 0.3 \left[\int_0^k qE(q)dq \right]^{1/2} \sim \left[k^2 E(k)\right]^{1/2}, \quad t_E^{-1} = k \left\langle U^2 \right\rangle^{1/2}$$

with relation between Lagrangian and Eulerian velocities

$$v_L(\mathbf{r}_0, t) \equiv \partial_t \mathbf{r}(t, \mathbf{r}_0) = v(\mathbf{r}(t, \mathbf{r}_0), t) \,.$$

This gives the generalization to unequal time correlations for Alfven velocity

$$\left\langle b_i(\mathbf{k},\tau')b_j^*(\mathbf{q},\tau)\right\rangle = \theta(\tau_H - \chi\tau_E(k,\tau))\exp\left[-\frac{(\tau'-\tau)^2}{\tau_E^2(k,\tau)}\right]\frac{(2\pi)^6}{4\pi k^2}\delta^3(\mathbf{k}-\mathbf{q})$$

$$\left[P_{ij}(\mathbf{k})E_B(\mathbf{k},\tau) - i\epsilon_{ijl}\frac{k^l}{k}h_B(\mathbf{k},\tau)\right],$$

and analogously for solenoidal velocity field

$$\left\langle v_i^S(\mathbf{k},\tau')v_j^{S*}(\mathbf{q},\tau)\right\rangle = \theta(\tau_H - \chi\tau_E(k,\tau))\exp\left[-\frac{(\tau'-\tau)^2}{\tau_E^2(k,\tau)}\right]\frac{(2\pi)^6}{4\pi k^2}\delta^3(\mathbf{k}-\mathbf{q})$$

$$\left[P_{ij}(\mathbf{k})E_V(\mathbf{k},\tau) - i\epsilon_{ijl}\frac{k^l}{k}h_V(\mathbf{k},\tau)\right],$$

where timescales are now conformal with τ_H the Hubble time.

i.e. $a\tau_E = t_E$ is the conformal Eulerian eddy turnover time, τ_H is the conformal Hubble time and $\chi \sim 1$ parameterizes the uncertainty in defining a cutoff criterion.

For compressible modes we anticipate

$$\left\langle v_D(t,k) v_D(t',k) \right\rangle = \left\langle v_D(t,k) v_D(t,k) \right\rangle \exp\left[-\frac{1}{2} \left(\frac{t-t'}{t_E(k)} \right)^2 \right] \cos\left[c_A k (t-t') \right] ,$$

with

$$c_A = \frac{\omega}{k} = \left(\frac{c_s^2 + v_A^2}{1 + v_A^2} \right)^{1/2} ,$$

Unequal Time Correlation

$$\langle v(\mathbf{k},\tau')v(-\mathbf{k},\tau'')\rangle \propto \langle v(\mathbf{k},\tau')v(-\mathbf{k},\tau')\rangle f(k,|\tau'-\tau''|) \qquad (5)$$

- typical Ansatz for f: $f(k,|\tau'-\tau''|) \approx \exp\left(-[|\tau'-\tau''|/\tau_E(k)]^2\right)$
- energy transfer in turbulence driven by time scale $\tau_E(k) \propto k^{-2/3}$
- Ansatz can lead to negative energies in GW spectrum (Caprini et. al. 2009)
- negative values due to $\cos(k|\tau'-\tau''|)$ factor
- Suggested Ansatz $f(k,|\tau'-\tau''|) \approx \theta(c - k|\tau'-\tau''|)$ and $c \lesssim \pi/2$
- However difficulty mostly resolved if $\tau_E(k) \propto k^{-1}$
- Sweeping effect: $\tau_E(k) \propto k^{-1}$ (Kraichnan 1965, Favre 1965)
- Swept-wave effect for compressible motion (Li et. al. 2013)

Swept wave model

- for dilatational modes (e.g. sound waves) decorrelation differs
- for sound waves need to account for wave behavior
- wave approximation $\langle v^d(t,k) v^d(t',k) \rangle \propto \cos\left(k c_s \delta t\right)$
- however need to account for decorrelation due to sweeping (Li et. al. 2013)
- swept wave approximation:
  $\langle v^d(t,k) v^d(t',k) \rangle \propto \cos\left(k c_s \delta t\right) \exp([t-t']^2 / t_E^s(k)^2)$

Gravitational Waves from MHD turbulence in phase transitions

Phase transitions can be characterised by the bubble nucleation rate β, which is roughly the inverse duration time of the phase transition, and the ratio of the latent heat and the radiation energy density, $\alpha = L/\rho_r$.
A star subscript refers to the time of the phase transition; $L_* \simeq 2H_*/(\beta v_w)$ is the integral scale of the turbulence.

Examples: Higgs portal model (Espinosa et al 2012), NMSSM

First order PT

- No standard model first order phase transition (FOPT)
- FOPT implies beyond the standard model physics
  - if standard model only approximate low temperature limit
    - implies higher order interaction terms (Buchmüller, Wyler 1986)
    - e.g. dimension six operators (e.g. ϕ^6) can lead to FOPT
  - additional scalar fields (e.g. Higgs portal) can lead to FOPT (Espinosa et. al. 2008)
  - general extensions like SUSY can lead to FOPT (Pietroni 1993)
  - additional dark sector phase transitions (Schwall 2015)
- FOPT also sources bulk motion and magnetic fields (Sigl et. al. 1996)
- FOPT will produce stochastic GW background
- LISA capable of constraining physics around $\sim$10 GeV to $\sim$100 TeV

Properties of FOPT

- Phase Transition parameters
  - latent heat α parameterizes strength
  - duration of transition β^{-1}
  - speed of bubble wall v_b
    - $v_b \lesssim c_s$ deflagration (Moore, Prokopec 1995)
    - $v_b \gtrsim c_s$ detonation (Steinhardt 1982)
- Thermal Phase Transition
  - $\alpha \lesssim 1$
  - Efficiency $\kappa(\alpha, v_b)$ peaks for $v_b \sim c_s$ (Espinosa et. al. 2010)
  - Initial bulk kinetic energy $\sim \alpha\kappa(\alpha, v_b)$
  - Turbulence important GW source (Kamionkowski et. al. 1994, Caprini et. al. 2009)
  - Sound waves as dominant source (Hindmarsh et. al. 2013)

Soundwaves or Turbulence

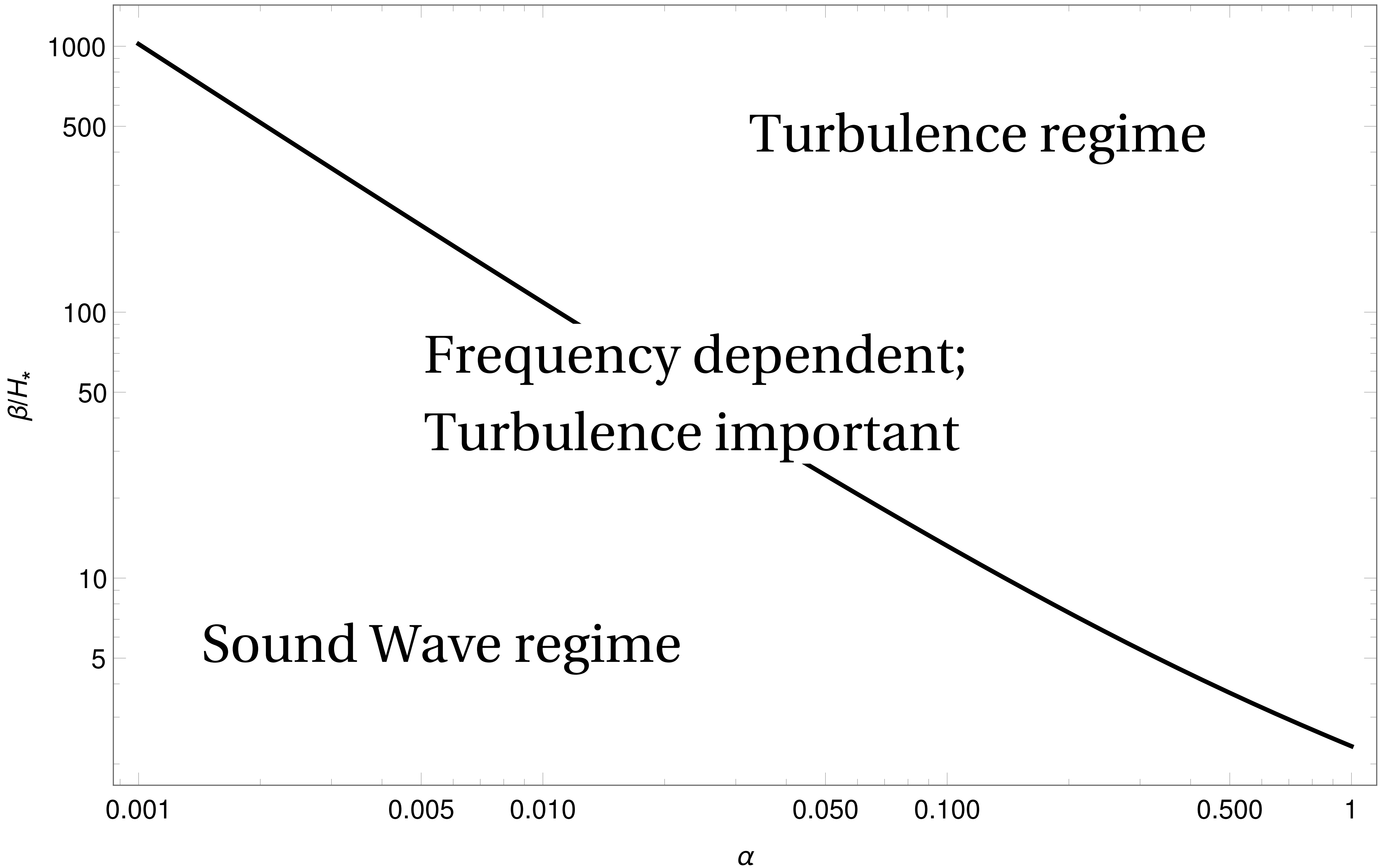

Assumptions for magnetic field and velocity spectra

magnetic and vortical kinetic spectra similar with Komogorov type spectra/ von Karman model

$$E_B(k,\tau) = [1 - f_D(\tau)]C_E \frac{K^5}{(c+K^2)^{17/6}} \theta(L_I/\lambda - K)\,,$$

with $K = kL_I/(2\pi)$, $c = 5/12$ giving a maximum at $K = 1$, $f_D(\tau)$ denoting the fraction of kinetic energy in dilatational modes, and λ being the dissipation scale. For the velocity spectrum we assume

$$E_V(k,\tau) = f_D(\tau) \frac{C_D K^5}{(c_D + K^2)^3} \theta(L_I/\lambda - K) + [1 - f_D(\tau)] \frac{C_E K^5}{(c+K^2)^{17/6}} \theta(L_I/\lambda - K)\,.$$

The vortical modes thus have the spectrum $\propto k^{-2/3}$ and the dilatational modes have a spectrum $\propto k^{-1}$ for $k > k_I$.
We use several models for the function $f_D(\tau)$.

One then gets expressions such as

$$
\begin{aligned}
\rho_{GW}(\mathbf{r},\tau) \approx \frac{G_{\rm N}\Omega_r f_g}{2\pi H_0^2}(\rho+p)^2 \int d^3\mathbf{k} \int d^3\mathbf{q} \int_{\tau_0}^{\tau} \mathrm{d}\tau' \int_{\tau_0}^{\tau'} \mathrm{d}\tau'' \, \frac{1}{q^3 p^3 \tau' \tau''} \cos(k(\tau'-\tau'')) \\
\times f_{\rm RSA}(\tau',\tau'',q) f_{\rm RSA}(\tau',\tau'',p) \Big[E_t^2(q,p,\tau') S^+(k,q,p) + 4H_t^2(q,p,\tau')(\hat{k}\cdot\hat{q})(\hat{k}\cdot\hat{p}) \\
+ S^-(k,q,p) \Big(4E_D(q,\tau')E_D(p,\tau')\cos\left[qc_s(\tau'-\tau'')\right] \cos\left[pc_s(\tau'-\tau'')\right] \Big) \\
+6D(k,p,q)E_S(q,\tau')E_D(p,\tau')\cos\left[pc_s(\tau'-\tau'')\right] \\
+6D(k,q,p)E_S(p,\tau')E_D(q,\tau')\cos\left[qc_s(\tau'-\tau'')\right] \Big].
\end{aligned}
$$

General scaling:

One has $\rho_{GW} \sim (\partial_\tau h)^2/G_N$ and $\partial_\tau h \sim G_N \rho_t t_H \sim \rho_t (G_N/\rho_{\rm dom})^{1/2}$, where ρ_t is the total energy density in magnetic fields and the velocity field and $\rho_{\rm dom}$ is the dominant total energy density during gravitational wave production. Combining this finally gives

$$\rho_{GW} \sim \frac{\rho_t^2}{\rho_{\rm dom}}\,, \quad \Omega_{GW} \sim \frac{\Omega_t^2}{\Omega_{\rm dom}}$$

where remarkably Newton's constant G_N has cancelled !

More detailed calculations based on the decorrelation models discussed above give somewhat different scalings,

$$\Omega_{GW}(\mathbf{k},\tau) \propto \Omega_{t,*}^{3/2} L_*^2 k^3 \quad \text{for} \quad k \ll k_I\,,$$

and a more complicated scaling with $\Omega_{t,*}$ for $k \gg k_I$.

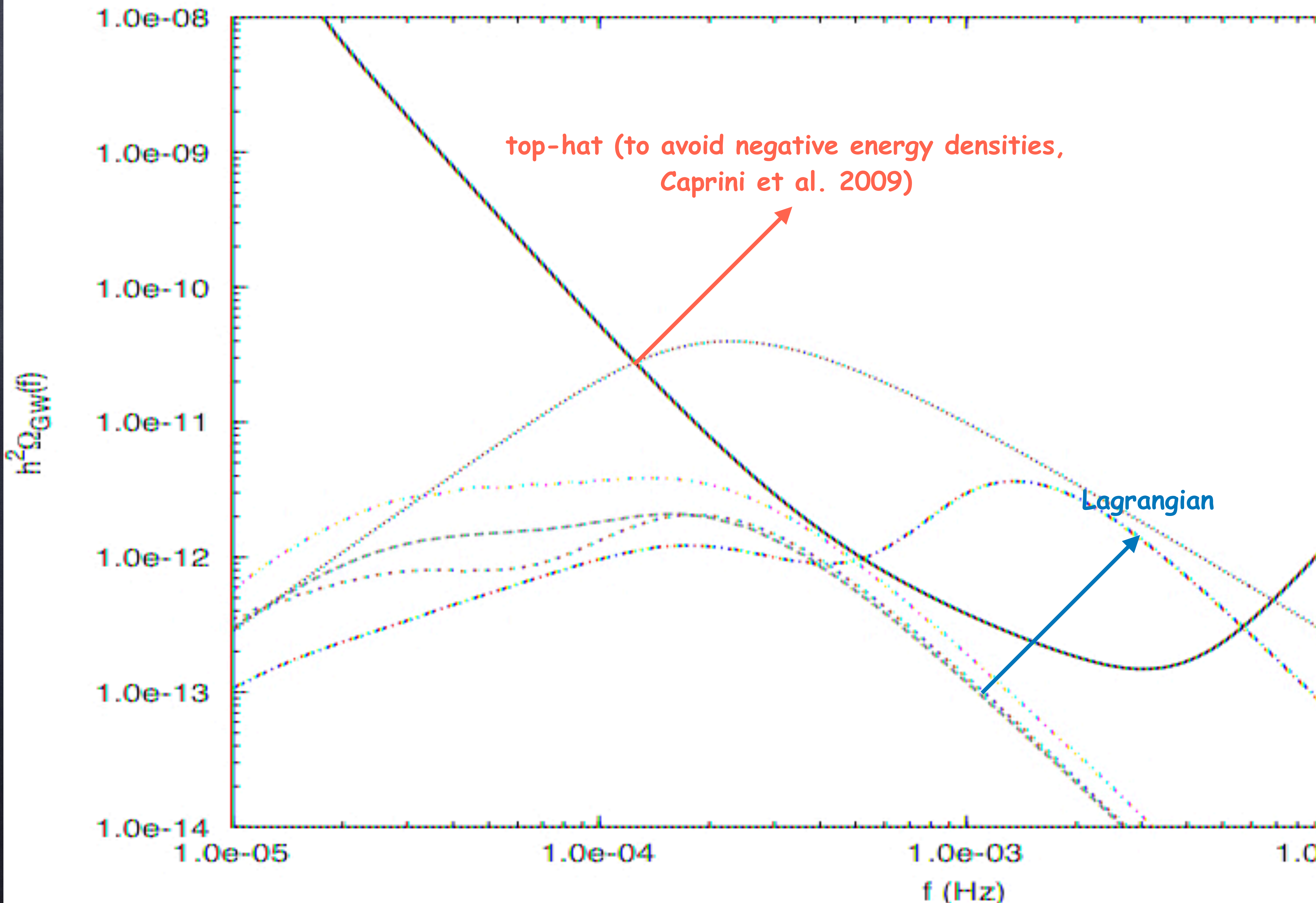
top-hat (to avoid negative energy densities,
Caprini et al. 2009)
Lagrangian
1.0e-08
1.0e-09
1.0e-10
1.0e-11
1.0e-12
1.0e-13
1.0e-14
$h^2\Omega_{GW}(f)$
1.0e-05
1.0e-04
1.0e-03
f (Hz)

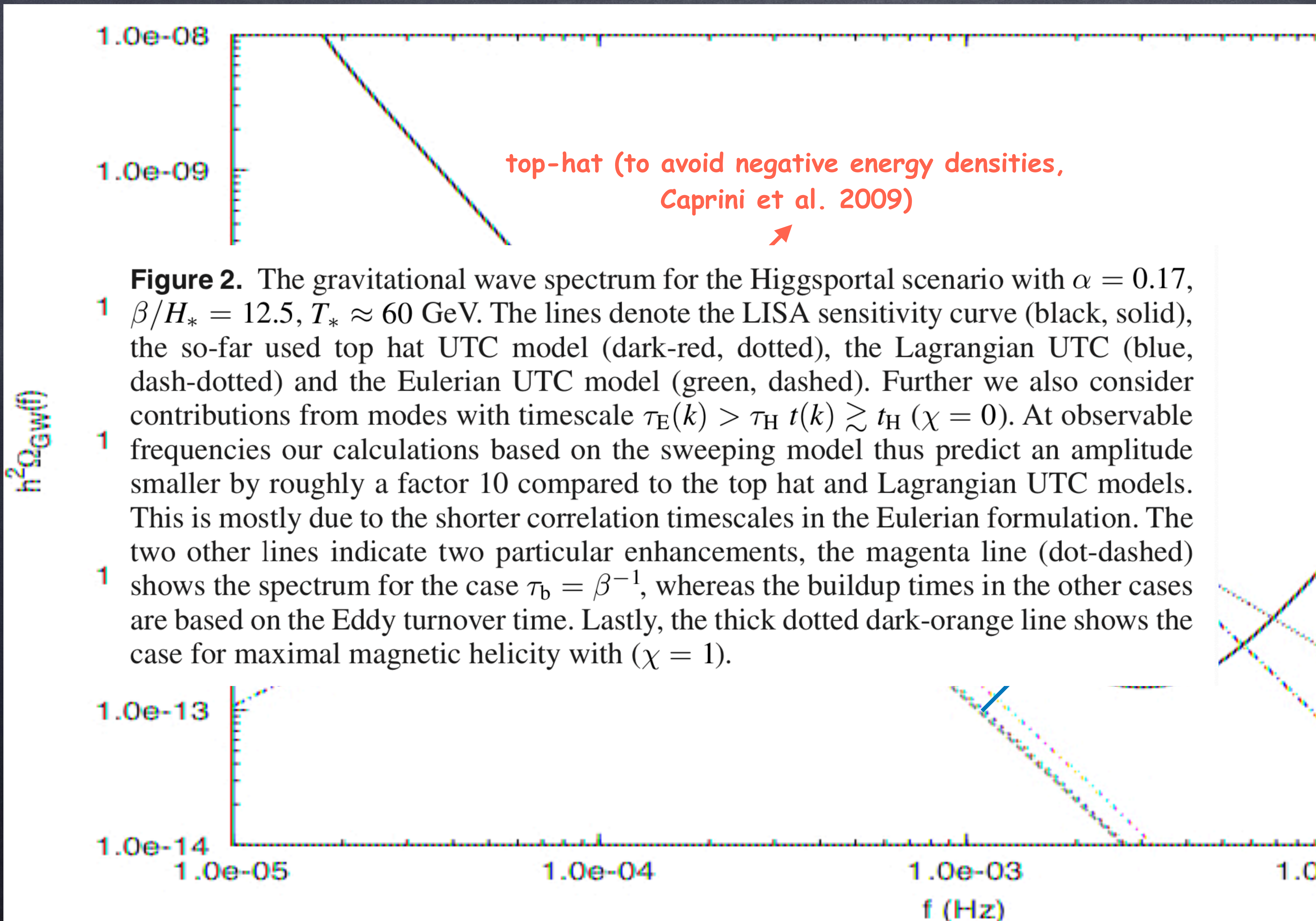

Figure 2. The gravitational wave spectrum for the Higgsportal scenario with $\alpha = 0.17$, $\beta/H_* = 12.5$, $T_* \approx 60$ GeV. The lines denote the LISA sensitivity curve (black, solid), the so-far used top hat UTC model (dark-red, dotted), the Lagrangian UTC (blue, dash-dotted) and the Eulerian UTC model (green, dashed). Further we also consider contributions from modes with timescale $\tau_E(k) > \tau_H \; t(k) \gtrsim t_H \; (\chi = 0)$. At observable frequencies our calculations based on the sweeping model thus predict an amplitude smaller by roughly a factor 10 compared to the top hat and Lagrangian UTC models. This is mostly due to the shorter correlation timescales in the Eulerian formulation. The two other lines indicate two particular enhancements, the magenta line (dot-dashed) shows the spectrum for the case $\tau_b = \beta^{-1}$, whereas the buildup times in the other cases are based on the Eddy turnover time. Lastly, the thick dotted dark-orange line shows the case for maximal magnetic helicity with ($\chi = 1$).

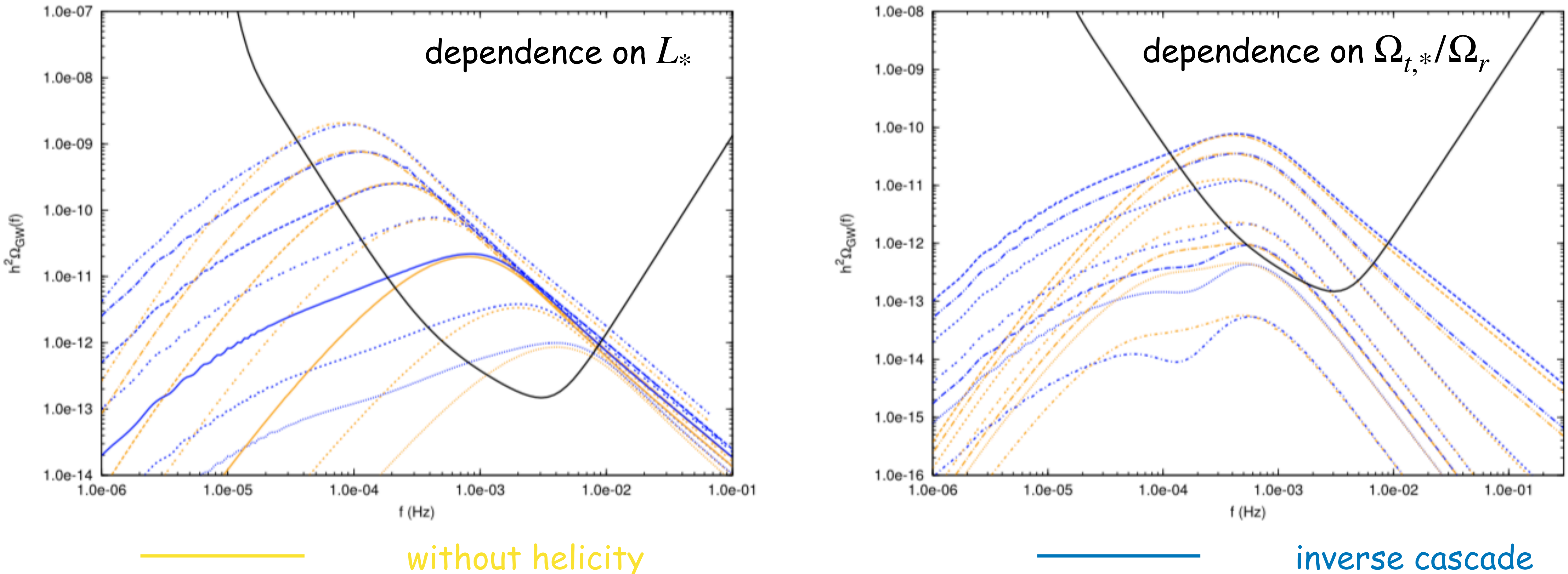

Figure 5. On the left panel, the dependence of the spectrum on the initial value L_* is shown, where $\Omega_{t,*}/\Omega_r = 0.2$ ($\alpha \sim 0.7$) and $T_* = 100$ GeV have been chosen. From top to bottom the lines correspond to $L_*H_* = 0.4, 0.2, 0.1, 0.05, 0.025, 0.01, 0.005$, where blue lines denote the helical case, while orange lines denote the non-helical case. On the right panel, the dependence on $\Omega_{t,*}$ is investigated for $L_*H_* = 0.1$ ($\beta/H_* \sim 20$). We show again both the helcial (blue) and nonhelical (orange) scenario. From top to bottom the lines correspond to $\Omega_{t,*}/\Omega_r = 0.2, 0.15, 0.1, 0.05, 0.035, 0.025, 0.01$. In both plots we have fixed $\chi = 2$ (only modes with $\chi\tau_E(k) < \tau_H$ contribute).

different models for conversion of sound waves into incompressible modes
and build-up of dilatational modes, $\alpha = 0.5\,, \beta/H_* \sim 10$

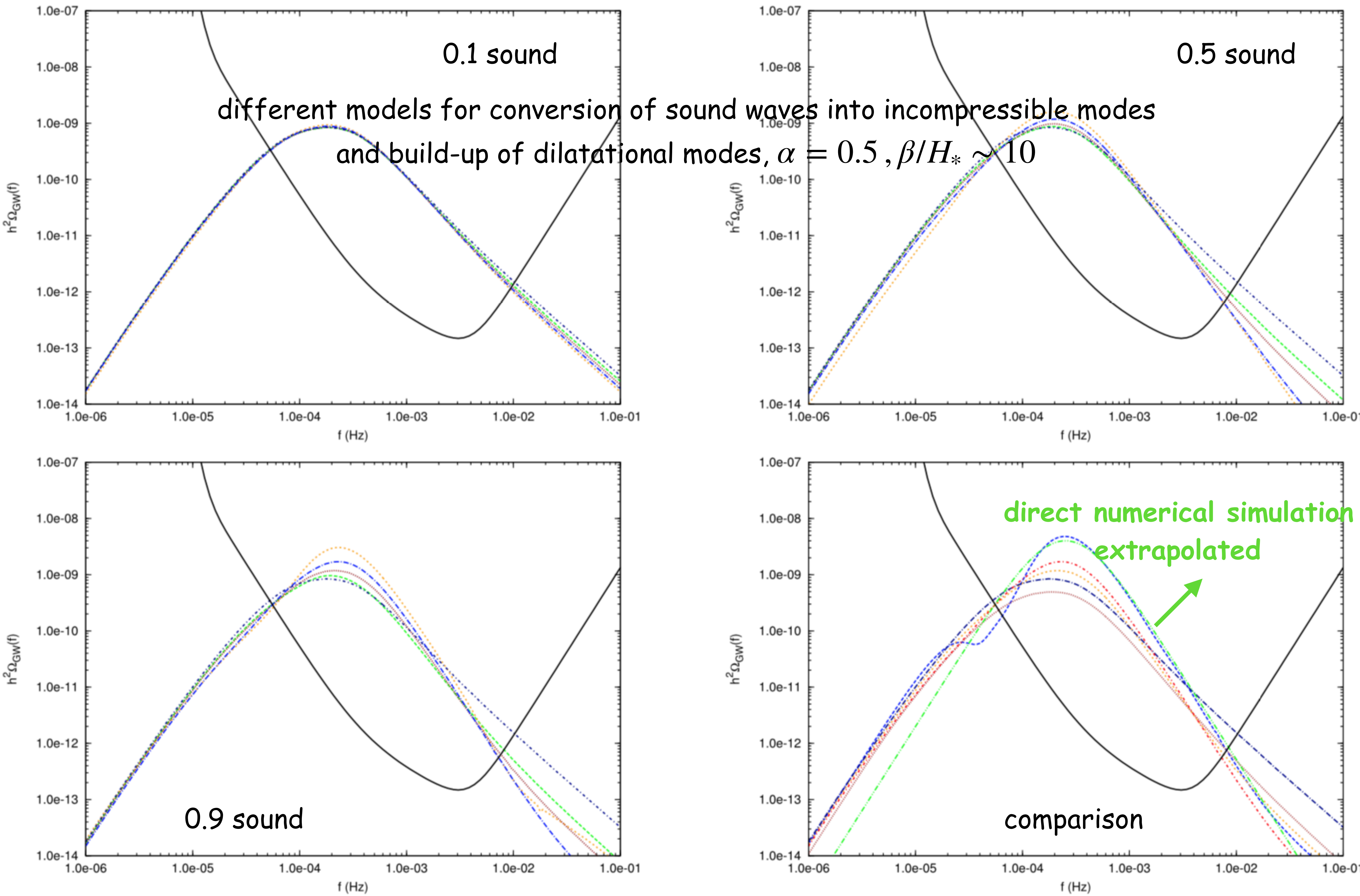

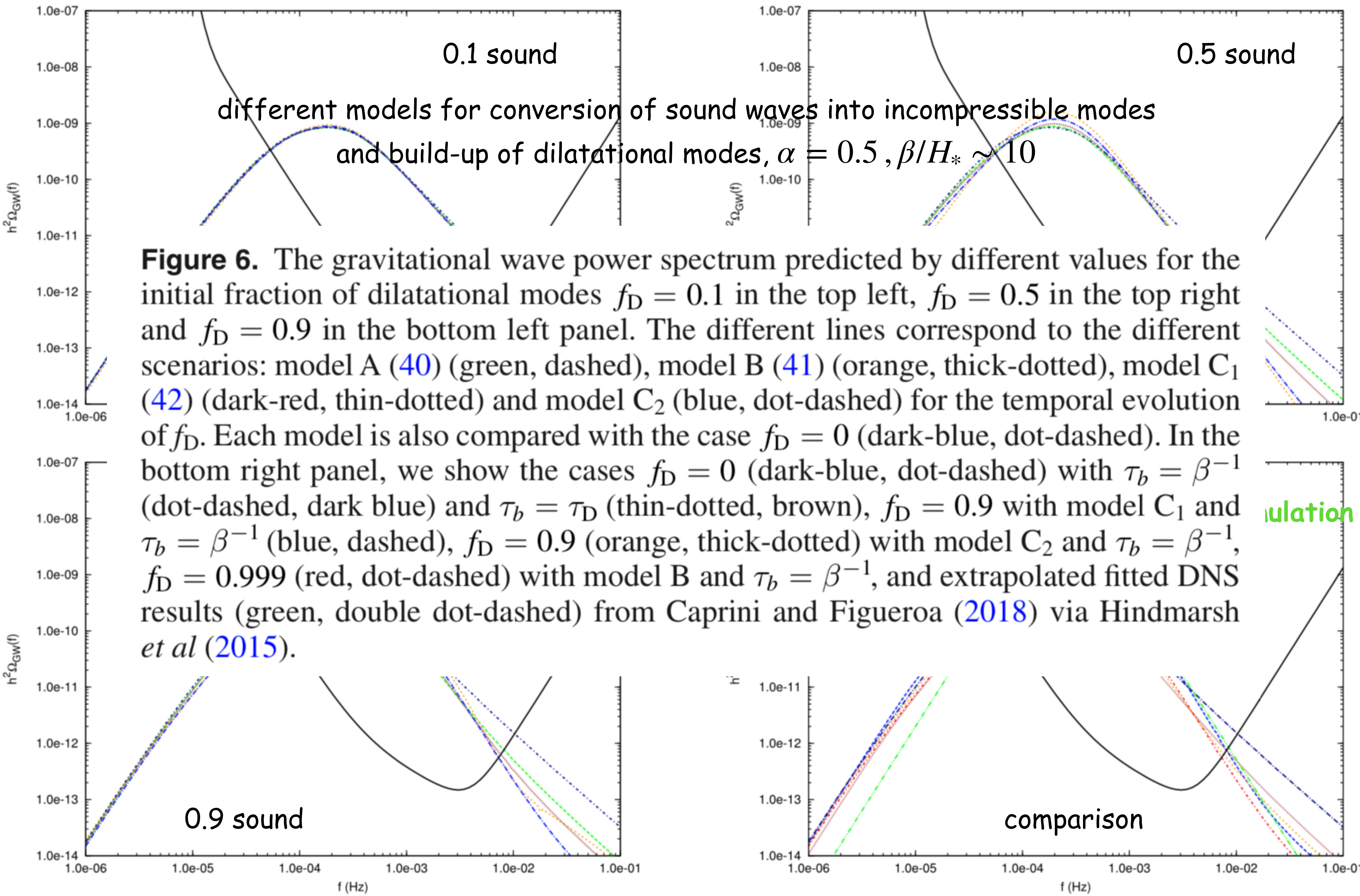

Figure 6. The gravitational wave power spectrum predicted by different values for the initial fraction of dilatational modes $f_{\rm D} = 0.1$ in the top left, $f_{\rm D} = 0.5$ in the top right and $f_{\rm D} = 0.9$ in the bottom left panel. The different lines correspond to the different scenarios: model A (40) (green, dashed), model B (41) (orange, thick-dotted), model C_1 (42) (dark-red, thin-dotted) and model C_2 (blue, dot-dashed) for the temporal evolution of $f_{\rm D}$. Each model is also compared with the case $f_{\rm D} = 0$ (dark-blue, dot-dashed). In the bottom right panel, we show the cases $f_{\rm D} = 0$ (dark-blue, dot-dashed) with $\tau_b = \beta^{-1}$ (dot-dashed, dark blue) and $\tau_b = \tau_{\rm D}$ (thin-dotted, brown), $f_{\rm D} = 0.9$ with model C_1 and $\tau_b = \beta^{-1}$ (blue, dashed), $f_{\rm D} = 0.9$ (orange, thick-dotted) with model C_2 and $\tau_b = \beta^{-1}$, $f_{\rm D} = 0.999$ (red, dot-dashed) with model B and $\tau_b = \beta^{-1}$, and extrapolated fitted DNS results (green, double dot-dashed) from Caprini and Figueroa (2018) via Hindmarsh *et al* (2015).

Summary

magnetic helicity strongly impacts the shape of the spectrum at low frequencies

for purely incompressible turbulence a power law scaling $f^{-5/3}$ for large $\Omega_{t,*}$ and $f^{-8/3}$ for small $\Omega_{t,*}$ is observed

for a strong first order phase transitions the high frequency tail of Ω_{GW}, scales as f^{-2} due to the sweeping effect of solenoidal modes on dilatational modes

direct extrapolation of the GW sourcing by sound-waves may lead to an overestimate of the gravitational wave energy density, since even a minor fraction ~ 0.1 of solenoidal modes will greatly reduce the GW production efficiency of sound-waves over a Hubble time for phase transition scenarios with a causal eddy turnover time

Outlook

- production rate of GW spectrum can become slightly negative (~1 %)
- requires improved modelling of decorrelation
- magnetic helicity (inverse cascade) still poses issues in modeling
- full inclusion of compressible MHD still lacking
- electroweak contribution during phase transition not yet simulated
- inclusion of MHD effects on decorrelation (e.g. magnetic sweeping)
- swept wave model also requires decorrelation timescale due to compressible motion
- spectra around peak most relevant and must be simulated in more detail